Nucleon Momentum Distributions in Deuterium and Carbon Inferred from Proton Scattering*†

J. B. CLADIS, W. N. HESS, AND B. J. MOYER
Radiation Laboratory, Department of Physics, University of California, Berkeley, California
(Received March 19, 1952)

Nuclear internal momentum distributions of deuterium, carbon, and oxygen are inferred from the energy distributions of the protons obtained at various scattering angles when 340-Mev protons are incident on these nuclei. The energy spectra of the protons from deuterium agree with the spectra obtained theoretically by using the deuteron nucleon momentum distribution given by the Fourier transform of the Hulthén wave function. Unfortunately, the experimental method is not so good as to distinguish differences in the portion of the deuteron wave function within the potential interaction. Protons obtained from carbon and oxygen have energy spectra that are consistent with the use of a Gaussian nucleon momentum density distribution having a $1/e$ value corresponding to a nucleon energy of 16±3 Mev.

Proton yields from deuterium nearly equal those expected from free proton-nucleon collisions. Oxygen gives proton yields in the spectral regions investigated that are 16/12 times the corresponding yields from carbon.

I. INTRODUCTION

EFFECTS of nucleon momentum distributions in nuclei manifest themselves in nearly every experiment that is performed using bombarding nucleons or gamma-rays of energies greater than about 100 Mev. Therefore, in addition to the pure theoretical interest of these distributions, their effective values are required before other aspects of experimental results can be inferred.

A momentum distribution[1] of the protons in carbon nuclei has been used by Chew and Goldberger[2] in conjunction with their "pick-up" process to explain the angular and energy distributions of the deuterons found by Hadley and York[3] when 90-Mev neutrons were incident on carbon. This momentum distribution was also found to be suitable by Lax and Feshbach[4] in interpreting the meson energy spectra from carbon at 90° obtained by Steinberger and Bishop[5] using the 330-Mev bremsstrahlung spectrum of the Berkeley synchrotron. However, Chew and Goldberger readily acknowledge in their paper that the very high momentum components in their postulated distribution should not be believed. Indeed, Henley and Huddlestone[6] find that the meson energy spectra from carbon at 90° resulting from proton bombardments[7,8] are not compatible with the high momentum components of the Chew-Goldberger distribution. These authors postulate a Gaussian momentum density distribution of the nucleons in carbon that has a $1/e$ value at a momentum corresponding to an energy of 19.3 Mev; this distribution also fits the low momentum points given by Chew and Goldberger.

A more direct method of inferring internal nuclear momentum distributions suggests itself with the advent of quite monoenergetic, high energy proton beams. Since the De Broglie wavelengths of bombarding nucleons having energies greater than about 100 Mev are quite comparable with the dimensions of the nucleon volume in nuclei, it is sensible to think of these nucleons as colliding with individual nucleons of target nuclei. Moreover, since the total scattering mean free path of nuclear material at these energies is of the order of the dimensions of light nuclei,[9] more than one-half of the scattered particles originate from single collisions within nuclei. The special name "quasi-elastic scattering" has been proposed to distinguish this important process which prevails at high energies when scattering angles greater than about 20° are viewed. This term is chosen to imply that the process is inelastic in that a rearrangement of the nucleus is brought about, but that it is elastic in the sense that a nucleon-nucleon collision occurs in the nucleus that resembles the scattering of nucleons by free target nucleons. The momentum distribution of the nucleons in a nucleus is related to the momentum distribution of the nucleons that are quasi-elastically scattered.

Wolff[10] has developed an equation that gives the energy spectrum of the nucleons scattered at a given angle as an integral over the nucleon momentum distribution. He deduced this equation by using the Born approximation and suitably averaging over the possible collisions of incident nucleons with nucleons

* Based, in part, on a dissertation submitted by one of the authors (JBC) to the University of California in partial fulfillment of the requirements for the degree of Doctor of Philosophy.
† This work was performed under the auspices of the AEC.

[1] The Chew-Goldberger momentum density distribution is

$$|N(k)|^2=\alpha/[\pi^2(\alpha^2+k^2)^2],$$

where k is the nucleon momentum and α is a momentum corresponding to a nucleon energy of 18 Mev.

[2] G. F. Chew and M. L. Goldberger, Phys. Rev. **77**, 470 (1950).
[3] J. Hadley and H. F. York, Phys. Rev. **80**, 345 (1950).
[4] M. Lax and H. Feshbach, Phys. Rev. **81**, 189 (1951).
[5] J. Steinberger and A. S. Bishop, Phys. Rev. **78**, 494 (1950).
[6] E. M. Henley and R. H. Huddlestone, Phys. Rev. **82**, 854 (1951).
[7] C. Richman and H. A. Wilcox, Phys. Rev. **78**, 496 (1950).
[8] Block, Passman, and Havens, Phys. Rev. **83**, 167 (1951).
[9] Fernbach, Serber, and Taylor, Phys. Rev. **75**, 1352 (1949).
[10] P. A. Wolff, thesis, University of California Radiation Laboratory Report No. 1410 (1951); Phys. Rev. **87**, 434 (1952).

possessing momentum that can contribute to the scattering of the nucleons into particular solid angles in the laboratory system. His result is

$$\frac{d^2\sigma}{d\Omega dE}=2\int_K^\infty \frac{|N(k)|^2}{|\mathbf{p}-\mathbf{q}|}\sum_{i=1}^{n}\sigma_i\frac{M}{\hbar^2}kdk,$$

where $K\cong|q-p\cos\theta|q|\mathbf{p}-\mathbf{q}|$, $|N(k)|^2$= the momentum density distribution of the nucleons in the nucleus; p= momentum of incident nucleon; q= momentum of scattered nucleon observed; k= momentum of nucleon in nucleus; θ= laboratory scattering angle; σ_i= differential cross section for scattering by ith nucleon of nucleus containing n nucleons; and M= nucleon mass. The approximation made in obtaining the result in such a simple closed form is small in comparison with the error inherent in the use of the Born approximation. Wolff also showed that protons that encounter two collisions with nucleons before emerging from nuclei do not appreciably alter the shapes of the spectra at energies greater than those at the maxima of the distributions.

The nucleon-nucleon nature of collisions involving high energy nucleons on nuclei is well illustrated by an experiment performed by Chamberlain.[11] He obtained the angular correlations of the two protons arising from collisions involving 340-Mev incident protons and protons in light nuclei. One counter was fixed to view protons scattered at 45°; the collision partners were viewed simultaneously by another counter that was varied in angle about the vicinity of the angular correlation obtained when protons are incident on free protons (90° nonrelativistically). The distribution of the proton angular correlations obtained by using a Li target compared to that obtained from an H target was found to have a greater width and to be peaked at an angle that was smaller by about 6°. The greater width is attributed to the momentum distribution of the target protons. The displacement of the peak by 6° can be explained by energy losses of the two protons after the collision sufficient to account for the binding energy of a proton in Li^7 and a small amount of excitation energy of the residual nucleus.

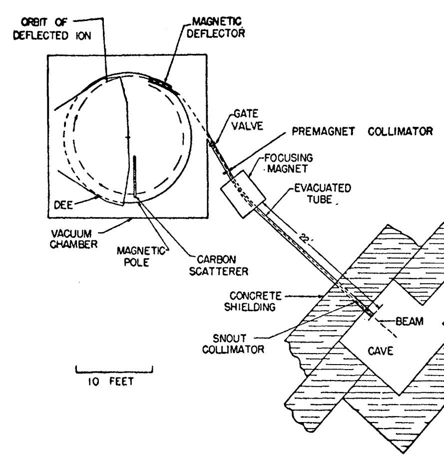

FIG. 1. A schematic diagram of the Berkeley 184-inch cyclotron and the path of the external beam.

This report concerns the energy spectra of protons scattered by H, D, C, and O at angles of 30° and 40°. These angles were chosen so that the nuclear diffraction scattering[12] would be negligible in comparison with the scattering due to quasi-elastic collisions. Wolff's theoretical spectra are used to infer nucleon momentum distributions in deuterium and carbon. The forms of the curves certainly reveal the prevalence of quasi-elastic scattering. The peaks of the spectra from carbon fall at slightly lower energies than those of the corresponding spectra from hydrogen, the differences being qualitatively explained by nuclear well and excitation effects.

II. EXPERIMENTAL METHOD

A. Energy Spectra

The spectra of the protons scattered by target nuclei are obtained by means of a magnetic deflection device, a so-called 35-channel magnetic particle spectrometer. The layout of the spectrometer as set up in the experimental area (cave) is shown in Fig. 2. In this figure the dimensions of some of the components are exaggerated to emphasize their effects on the resolving power of the spectrometer. These effects will be discussed in the next section.

1. Proton Beam

The external 340-Mev proton beam of the Berkeley 184-inch synchrocyclotron is used. This beam is pulsed at a repetition rate of about 66 per second. In order to reduce the number of accidentals in the detection counters for a given counting rate it is necessary to use a large beam pulse width. A maximum width of about 15 to 20 microseconds is obtained by scattering[13] the protons out of the circulating orbits of the cyclotron (see Fig. 1). The energy spectrum of this beam, which is calculated as indicated in Sec. III to have a width at half-height of about 11 Mev, must be taken into consideration in the interpretation of the experimental spectra. The cross section of the beam in the cave is limited to be rectangular, $1\frac{3}{8}$ inches wide and $\frac{3}{4}$ inches high, by a brass collimator located at the exit end of the evacuated tube (see Fig. 1).

2. Targets

As shown in Fig. 2 the targets used are narrower than the beam cross section. However, they are taller than the vertical beam dimension so that a fixed length

[11] O. Chamberlain, private communication.

[12] Richardson, Ball, Leith, and Moyer, Phys. Rev. **86**, 29 (1952).

[13] C. E. Leith, Phys. Rev. **78**, 89 (1950).

of the targets is intercepted by the beam. The cross sections of the targets in the horizontal plane are forced to be parallelograms by the conditions: (1) the targets are required to be narrow with respect to the width of the beam so that the energy spread of the incident protons striking the targets shall be small, as described in detail in Sec. III, and (2) the target dimension perpendicular to the direction of the observed scattered particles is required to be small to achieve good energy resolution, since this dimension is in effect the width of the first slit of the spectrometer.

Energy spectra are obtained of protons scattered from targets of water, heavy water, carbon, polyethylene, container, and air blanks. Subtractions are required to obtain proton spectra from hydrogen, deuterium, and oxygen. Since equal average proton energy loss in the targets used greatly facilitates these subtractions, and since the stopping powers of these targets are not the same, the target dimensions in the direction of the scattered particles observed are varied to achieve this equal average energy loss condition. A knowledge of the integrated beam per target that is required to effect the subtractions is obtained by setting an argon-filled ionization chamber in the beam as shown in Fig. 2.

3. Particle Spectrometer

The scattered particles detected enter the corner of a rectangular magnetic field through a "slit" proportional counter (see Fig. 2). This counter has an active area whose width is $\frac{1}{8}$ in. The particles then traverse two more proportional counters located in the magnetic field. They afterwards encounter an array containing 35 Victoreen G-M tubes before traversing the final proportional counter located in back of the G-M tubes. Energy channels of the spectrometer are defined by the target considered as the first slit, the slit counter, and the G-M tubes. Thirty-five channels are used so that nearly the entire spectra can be obtained with a single field setting and with a constant arrangement of the spectrometer components.

The G-M tube signals giving the distribution of particles in the energy channels are properly amplified and recorded on a bank of 35 registers. To reduce the accidental coincidences due to random background, the G-M tube amplifiers are gated "on" by the quadruple coincidences of the proportional counter signals. These quadruple coincidences also serve as a convenient means of arriving at the relative integrated yields of protons from targets at the scattering angles of observation.

4. Nature of Scattered Particles Detected

The spectrometer described above gives merely the momentum distribution of the particles analyzed, since only their bending effect in the magnetic field is observed. The masses of the particles must be known to deduce their energy spectra from the momentum

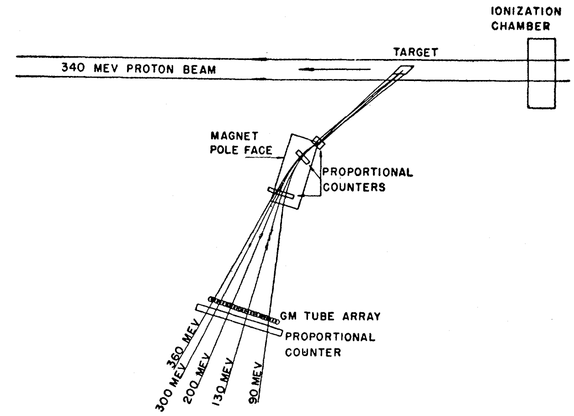

FIG. 2. The magnetic deflection spectrometer used to obtain the proton energy spectra.

distributions. However, the great preponderance of these particles is expected to be protons, particularly at the scattering angles used (30° and 40°). This expectation arises from the considerations embodied in the introduction concerning the De Broglie wavelengths of the bombarding protons, the transparency of light target nuclei, and the investigations by Hadley and York[3] of the secondary particles knocked out of target nuclei by 90-Mev incident neutrons in which the only ionizing particles detected were protons, deuterons, and tritons. The pick-up theory accounts well for the angular ane energy distributions of the deuterons and tritons. The tritons were observed in small numbers and only in the near forward direction. Heidmann[14] considers the energy dependence of the pick-up process and shows that the total cross section for the production of deuterons at 300 Mev is down to less than a thousandth of its value at 100 Mev. Moreover, he shows that the angular distribution becomes increasingly peaked in the forward direction as the incident energy becomes larger. The number of deuterons produced by 340-Mev protons at scattering angles of 30° and 40° should be quite small indeed.

Alpha-particles are certainly ejected in spallation reactions, but they require 100 Mev to be recorded in the lowest energy channel. Alpha-particles in the spallation products resulting from 340-Mev proton bombardments rarely possess energies greater than about 30 Mev.[15] Mesons require energies greater than 300 Mev to be recorded in the lowest energy channel. Clearly, mesons of this energy are not produced by the proton beam.

Thus, only deuterons would conceivably contaminate the energy spectra calculated on the assumption that protons alone are detected. These deuterons are found to be quite negligible in number, if present at all, by a method described in Sec. III of finding the pulse heights of the particles in various magnet channels.

[14] J. Heidmann, Phys. Rev. **80**, 171 (1950).
[15] R. Batzel, private communication.

B. Absolute Cross Sections

Relative yields are obtained, as stated before, from the proportional counter quadruple coincidences data. In principle, they could be obtained from the areas of the proton spectra; but this method is not feasible since the proton spectrum from hydrogen is sharp, and its apparent shape is simply the resolution pattern of the spectrometer which is contained within only a few channels.

The absolute cross sections for protons from deuterium can be obtained at each scattering angle by comparing the proton yields from deuterium to the corresponding proton yields from hydrogen and using the proton-proton differential scattering cross section at 340 Mev given by Chamberlain, Segrè, and Wiegand.[16] In the case of protons from carbon, these comparisons give only estimates in the nature of lower limits for the cross sections, since the proportional counters do not accept the complete energy breadth of the spectrum. Low energy components below about 90 Mev are not included.

III. CALIBRATION OF PARTICLE SPECTROMETER

A. Resolving Power of Particle Spectrometer

The resolving power of the spectrometer is obtained by "folding" together the individual resolving power curves of the components which affect the energy resolution. These components are (1) the target width considered as a slit, (2) the width of the slit counter, (3) the width of the G-M tubes, (4) the energy losses of the protons in the targets, and (5) the small angle scattering in the proportional counter windows and in the air path. In practice the resolving power curves of these components are approximated by rectangles, and are referred to, for simplicity, as the energy widths of the components.

The energy width of a particular component is found by assuming the widths of all the other components to be zero. For example, the energy width of a G-M tube is the maximum energy difference of two protons that can still be accepted by a certain G-M tube when assuming that the protons originate at the center of the target, suffer no energy spread in emerging from the target, go through the center of the slit counter, and suffer no small angle scattering in the proportional counter windows or in the air path. Similarly, the energy width of the slit counter is given as the energy difference that would be recorded by point G-M tubes in juxtaposition at the G-M tube array, of two protons that have the same energy and that take the same path described above with the exception that one proton traverses the slit counter at one edge while the other proton traverses the opposite edge. The widths of the other components are obtained by using the same approach.

[16] Chamberlain, Segrè, and Wiegand, Phys. Rev. 83, 923 (1951).

All of the energy widths of the components are energy dependent. The G-M tubes define energy channels from about 350 Mev to 95 Mev. Between these limits the energy drops off almost exponentially as a function of position along the G-M tube array. Thus, the change in energy with respect to a fixed linear increment along this array is also nearly exponential. From this fact, it is clear that the energy widths of all of the factors mentioned above, except that due to the target thickness, become smaller as the proton energies become lower. The energy losses of the scattered protons in the target, of course, increase as the energies of the protons decrease. As a result of these effects, the resolving power curves of the energy channels decrease exponentially in width in the direction of lower energies until an energy E_0 is reached, after which the channel resolutions are limited by energy losses in the targets. At proton energies less than E_0, the energy resolution of the channels becomes progressively worse. The maximum resolving power of the spectrometer is, therefore, at the energy E_0. Parameters are chosen so that E_0 falls near the peaks of the spectra, where the best resolving power of the spectrometer is required.

A practical limit of the resolution is forced by the unavailability of an infinite amount of cyclotron time. A compromise between channel counting rates and energy resolution is necessary. After having decided the practical resolution that can be used, care must be taken that maximum channel counting rates are obtained consistent with this energy resolution. This condition can be met by making the energy widths of the slits (target and proportional counter) nearly equal to the energy widths of the G-M tubes in every energy channel.

The energy width due to small angle Coulomb scattering in the proportional counter windows is kept at a minimum by using 0.001-inch aluminum windows and by forming the confines of the "slit" proportional counter with 0.0005-inch aluminum.

The energy spread of the beam must be known before a comparison of theory to experiment can be made. This is obtained in an approximate manner by assuming a flat energy spectrum of protons scattered into the magnetic channel (refer to Fig. 1) from the circulating tank of the cyclotron. Then the energy distribution is found of the protons that can strike the target after passing through the cyclotron premagnet collimator and being bent through an angle of about 20° by the beam focusing magnet. It is clear that the problem of finding this distribution is the same as that of finding the resolving power of the spectrometer. In each case two collimating slits precede the magnet and one slit accepts the flux that has been deflected in the magnetic field. The energy widths that have to be folded together now are those due to (1) the magnetic channel opening, (2) the premagnet collimator, and (3) the target width. The resultant width at half-height is found to be about 11 Mev. No estimate has been made of the low energy components in the beam produced by scattering from the rectangular collimator preceding the target.

The resolving power of the spectrometer calculated above can be checked experimentally at energies corresponding to the peaks of the proton spectra from hydrogen. These spectra also indicate a small contribution of low energy components of the beam mentioned above to be incident upon the target. The experimental data representing a particular proton energy spectrum from hydrogen, whose peak falls at an energy E, should agree with the theoretical spectrum obtained by averaging the resolving power of the spectrometer at the energy E over the energy spread of the beam. Actually, the shapes of the proton spectra from hydrogen are experimentally quite unknown, the spectra being so sharp as to be contained in only a few channels. The comparisons at 30° and 40° are shown in Fig. 3. At 30° only a few experimental points are available to define the peak since the G-M tubes in the array were separated by $\frac{3}{16}$ in. They were in juxtaposition in the vicinity of the peak when the 40° data were taken. The areas of the calculated resolution curves are chosen to agree with the proton yields as obtained from the proportional counter data. The relative ordinate scale used in Fig. 3(a) does not correspond in any way to that chosen in Fig. 3(b).

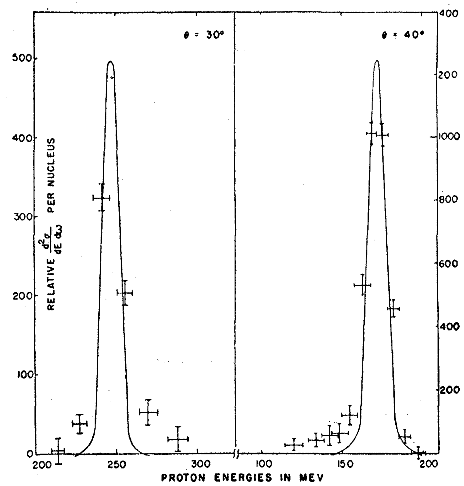

FIG. 3. Proton energy spectra at 30° and 40° from the scattering of 340-Mev protons by hydrogen.

B. Magnet Channel Energies

The magnet channel energies are obtained by using the fact that a wire carrying a current of I abamperes and subjected to a tension of T dynes in a magnetic field B will assume the trajectory of a charged particle whose energy corresponds to $B\rho = T/I$ gauss-centimeters. This can be shown very easily. A short length dl of a current carrying wire in a magnetic field subtending an angle $d\theta$ at a distance ρ from the center of curvature is acted upon by the radial force $BIdl$. If this segment is in equilibrium, this radial force must equal $2T(\frac{1}{2}d\theta) = Td\theta$, for $d\theta$ small. Using $\rho = dl/d\theta$, the very simple and useful result $B\rho = T/I$ is obtained. The wire follows the path of a constant energy particle since this relation holds at every point of the wire. The energies obtained in this way are in error by less than 2 percent.

If the magnet channel energies are also obtained analytically, assuming a constant field over the dimensions of the pole faces, these calculated energies differ from those obtained by means of the wire method by nearly 8 percent. By examining the field of the magnet along the paths of the particles, the discrepancies are well accounted for by the effect of the fringing field. It is also reassuring to note that at every scattering angle θ, the calculated proton energy obtained by assuming free equal mass particle collisions agrees, within the accuracy of the angle measurement (1°), with the peak of the experimentally obtained proton spectrum from hydrogen.

C. Test for Deuterons in Particles Measured by Spectrometer

The energy channels designed to accept protons from 90 Mev to 350 Mev can also accept deuterons in the energy range from 45 to 197 Mev. Deuterons arising from the elastic scattering of protons by the deuterons in the heavy water target have energies equal to $(8/9)T_0 \cos^2\theta$, nonrelativistically, where T_0 is the incident proton energy and θ represents the angles of the struck deuterons. At $\theta = 40°$ this energy is about 177 Mev, which corresponds to a proton channel energy of 317 Mev. According to Heidmann[14] the deuterons from the pick-up process have broad energy spectra that are probably peaked near the same energies as those of the recoil deuterons from elastic p-d collisions. An attempt was made, therefore, to distinguish deuterons from protons at the proton energy channels in the vicinity of 315 Mev.

Since the deuterons of 177 Mev produce pulses in proportional counters that are a factor of 2.5 higher than those produced by 317-Mev protons, a method of discrimination on the basis of pulse heights is at once suggested. This was attempted by seeking two voltage plateaus in fivefold proportional counter coincidences; the plateau at the higher voltage range should include protons and deuterons, that at the lower range should contain deuterons alone. A proportional counter was located to intercept proton flux in the energy range from 300 Mev to 340 Mev (deuterons of energy from 165 Mev to 190 Mev). It was placed behind the last proportional counter normally intercepting the particle flux being analyzed (see Fig. 2). Fivefold coincidences were then obtained between the signals of this counter and those of the usual counters producing the quads for the spectra, which were obtained concurrently with this data. These fivefold coincidences were recorded as a function of the voltage applied to the proportional

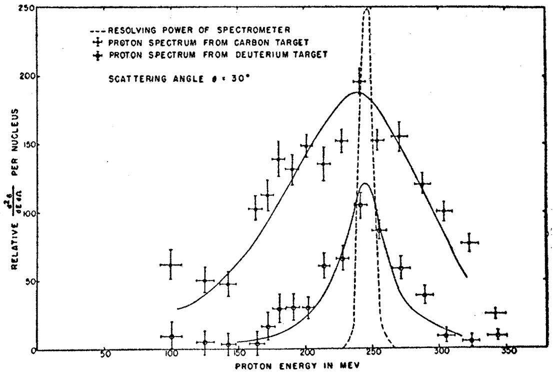

FIG. 4. Proton energy spectra at 30° from 340-Mev protons on deuterium and carbon. The calculated resolving power curve is shown dotted.

counter added. The data obtained in this way, using heavy water and water targets show that the deuterons constitute a very small fraction, if any at all, of the particles in these channels.

IV. ANALYSIS OF DATA

A. Channel Efficiencies

The magnet energy channels have widely varying efficiencies for accepting particle flux. If a flat spectrum of protons were viewed by the spectrometer, the number of counts in each channel would be proportional to the energy widths of the G-M tubes. The channel counts would decrease in a near-exponential manner from channel 1 to channel 32, the number of counts in channel 1 being about 9 times as great as that in 32. It is clear that these channel counts must be divided by the relative efficiencies (G-M tube widths) to reproduce the particle spectra.

The spectra would also be distorted somewhat by the target if it were so thick, and if the energy channels were so wide, that an appreciable difference would exist in the target energy losses of particles having energy differences equal to the widths of the channels. This would cause the spectra to be distorted because of the variation of its effect on the channel acceptance efficiencies. The correction due to this cause is quite negligible, however, since there exists a rather fortuitous compensating effect. As the stopping power of the target becomes more rapidly changing with energy (at the lower energy channels), the G-M tube widths of the channels become narrower in such a way that this target effect remains negligible in all of the channels.

B. Subtractions Made in Obtaining Spectra

The possibility of obtaining accidental coincidences in the cave is generally very high because of the intense radiation background. By lowering the beam intensity and by providing adequate shielding, the accidentals in the quadruple coincidences of the proportional counter signals were reduced to about one percent. Accidental coincidences were still found to occur, however, between the G-M tube signals and the gates applied to the G-M tube amplifiers. These accidentals were evaluated experimentally for each target used by obtaining a spectrum while applying gates to the G-M tube amplifiers which were random but restricted to beam pulses periods, and then subtracting the "real" components of the spectrum (obtained by using quadruple coincidences gates) which should have occurred for the same integrated beam.

The channel data are not divided by the channel efficiencies until the required normalizations, corrections, and subtractions are performed. These are all incorporated in the mathematical operations indicated below. The channel counts must first be corrected for the accidentals and for the no target (blank) contributions. Then the data are normalized to a per-target-mole basis to obtain the relative number of protons scattered by oxygen, deuterium, and hydrogen from the proper subtractions.

Let CH_2 = original channel counts from polyethylene target/beam monitor, C = original channel counts from carbon target/beam monitor, D_2O = original channel counts from heavy water target/beam monitor, H_2O = original channel counts from water target/beam monitor, A = original channel counts from air blank target/beam monitor, B = original channel counts from empty liquid container/beam monitor, g = number of gates/beam monitor), M = number of target moles/inch height of target in beam, and K = accidentals/gate. Let the subscripts hw, w, p, c, a, and k refer, respectively, to heavy water, water, polyethylene, carbon, air blank, and "can" blank. Then the following operations give the relative contributions of protons from the nuclei listed below.

Carbon (C): $(1/M_c)[\mathrm{C}-g_cK-(A-g_aK)]$,

Hydrogen (H_2):

$$(1/M_p)[\mathrm{CH_2}-g_pK-(A-g_aK)]-(\mathrm{C}),$$

Oxygen (O): $(1/M_w)[\mathrm{H_2O}-g_wK-(B-g_vK)]-(\mathrm{H_2})$,

Deuterium (D_2):

$$(1/M_{hw})[\mathrm{D_2O}-g_{hw}K-(B-g_kK)]-(\mathrm{O}),$$

Oxygen (O): $(1/M_w)[\mathrm{H_2O}-g_wK-(B-g_wK)]-(\mathrm{H_2})$.

The values used are

$$g_{hw}=67.4,\ g_p=54.9,\ g_k=5.76,\ M_{hw}=0.418,\ M_p=0.418,$$
$$g_w=63.2,\ g_c=58.6,\ g_a=2.81,\ M_w=0.390,\ M_c=0.655.$$

In order to obtain the integrated yields of protons from these nuclei using the quads, the same subtractions indicated above are performed with the simplification that now $K=0$.

VI. FINAL RESULTS

A. Presentation of Data

The proton spectra from carbon and deuterium at 30° and at 40° are shown in Figs. 4 and 5, respectively.

The calculated resolution curves that are fitted to the proton spectra from hydrogen as shown in Figs. 3(a) and 3(b) are reproduced in Figs. 4 and 5 so that the effects of internal momenta on the shapes and peaks of the spectra may be noted. The ordinates of the graphs representing the spectra are entirely relative. In addition, they are only consistent at a particular scattering angle; i.e., the relative ordinate scale used in representing the 30° data is not correlated with that used for the 40° data. The vertical lines at the experimentally obtained points indicate only standard deviations due to counting statistics. The horizontal lines depict the widths at half-height of the channel resolving power curves averaged over the beam energy spread. Since the channel acceptance energies are narrower than the target energy losses in the lower energy channels, the channels are combined until these widths are nearly the same. As far as the counting rates are concerned, this procedure similates the use of G-M tubes of adjustable physical widths such that their energy widths nearly equal the energy losses in the target at the central energies of the modified channels. The counting statistics in these channels thus become improved considerably with essentially negligible losses in energy resolution.

That these curves may more closely represent the proton spectra immediately following the collisions, the data are plotted at energies that are greater than the central channel energies by the mean energy losses in the target. This shift in energy corresponds to about 4 Mev at the peaks of the spectra.

B. Discussion of Results

The curves that are shown fitted to the spectral points of protons from deuterium and from carbon are the theoretical spectra obtained by inserting various momentum distributions into the equation given by Wolff, as is discussed in Sec. I. Of course, the energy resolution of the spectrometer is first folded into these theoretical curves before comparing them with the data.

The theoretical spectra of protons from deuterium

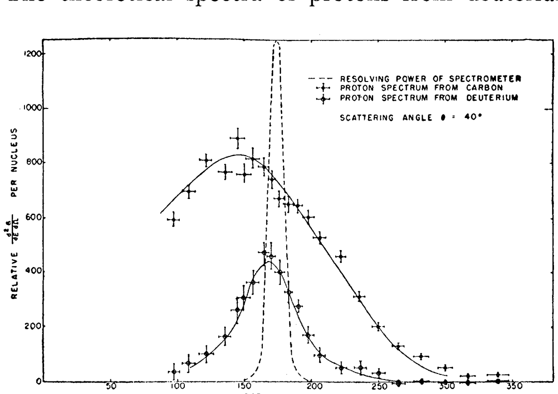

FIG. 5. Proton energy spectra at 40° from 340-Mev protons on deuterium and carbon. The calculated resolving power curve is shown dotted.

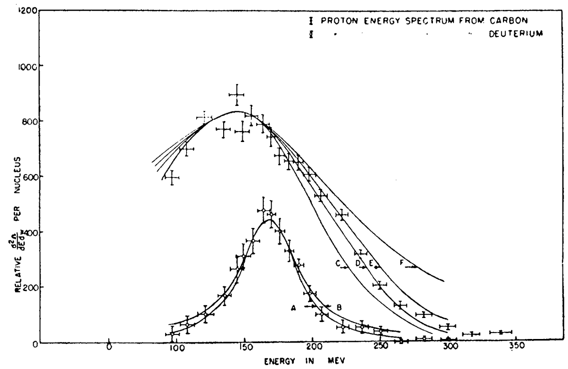

FIG. 6. The curves that are drawn to the 40° data depict the sensitivity of the theoretical proton energy spectra to the assumed nucleon momentum density distributions shown in Fig. 7.

drawn to the data in Figs. 4 and 5 are obtained by using the momentum density distribution given by the square of the Fourier transform of the Hulthén wave function,

$$(e^{-\alpha r}-e^{-\beta r})/r,$$

where $(\alpha h)^2=m\epsilon$ (m=nucleon mass, ϵ=deuteron binding energy) and $\beta/\alpha=7$. The numerical solution of the Schroedinger equation using the Yukawa potential is closely approximated by the function chosen above.[17] The value $\beta/\alpha=7$ is obtained from the effective range given by Blatt and Jackson[18] (see also Gluckstern and Bethe[19]).

In order that the sensitivity (or insensitivity) of this method to the portion of the deuteron wave function located within the interaction potential may be discerned, two theoretical curves obtained by using widely different wave functions are drawn to the 40° proton spectrum from deuterium in Fig. 6. Curve A is obtained from the Hulthén wave function described above; curve B is obtained by assuming the wave function $e^{-\alpha r}/r$, which holds properly in the region of no potential interaction, to hold everywhere. That Curve B is wider than curve A is understandable since the wave function $e^{-\alpha r}/r$ diverges at the origin, exaggerating the high momentum components in its transform. It can been seen, however, that the data do not divulge information concerning the wave function of the deuteron since appreciable differences in the curves occur only at the "tails" where the experimental data are not well known. Nevertheless, it is comforting to note that the theoretical curves fit the data as well as they do in this case of the deuteron for which the momentum distribution is fairly well established, and confidence is gained in the momentum distribution used to fit the proton spectrum from carbon.

A Gaussian momentum distribution containing a $1/e$ value at a momentum corresponding to a nucleon

[17] G. F. Chew, Phys. Rev. **74**, 809 (1948).
[18] J. Blatt and J. D. Jackson, Phys. Rev. **76**, 18 (1949).
[19] R. L. Gluckstern and H. A. Bethe, Phys. Rev. **81**, 761 (1951).

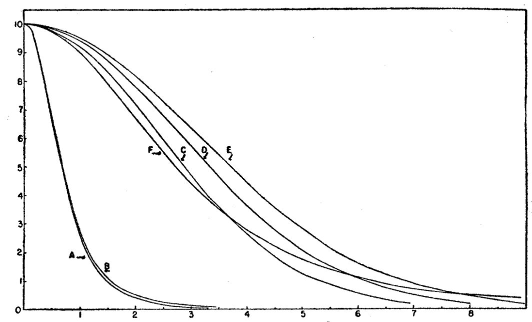

FIG. 7. Nucleon momentum density distributions that were used in attempts to fit the experimental data. These curves represent (A) the distribution given by the Fourier transform of the deuteron Hulthén wave function:

$$\left|\frac{1}{p^2+\alpha^2\hbar^2}-\frac{1}{p^2+\beta^2\hbar^2}\right|^2,\quad \alpha^2\hbar^2=m\epsilon,\quad \beta/\alpha=7;$$

(B) the distribution given by the transform of the deuteron $e^{-\alpha r}/r$ wave function $|1/(p^2+\alpha^2\hbar^2)|^2$, $\alpha^2\hbar^2=m\epsilon$; (C), (D), and (E) are Gaussian distributions $\exp(-p^2)/\alpha^2\hbar^2$, where $\alpha^2\hbar^2/2m$ equals 12 Mev, 16 Mev, and 20 Mev, respectively; and (F) the Chew-Goldberger distribution $|1/(p^2-\alpha^2\hbar^2)|^2$, $(\alpha^2\hbar^2/2m)=18$ Mev.

energy of 16 Mev has been used to give theoretical proton spectra from carbon that fit the 30° and 40° data as shown in Figs. 4 and 5. Figure 6 depicts the curves obtained when other momentum distributions are attempted to fit the 40° data. In obtaining curves C, D, and E, Gaussian momentum distributions having $1/e$ values corresponding to energies of 12, 16, and 20 Mev, respectively, have been used. Curve F is deduced from the Chew-Goldberger momentum distribution. The momentum density distributions used are plotted in Fig. 7 as functions of $P/(2m)^{\frac{1}{2}}$, so that the energies of the nucleons corresponding to specific regions of the distributions can merely be obtained by squaring the corresponding values of the abscissas (the relativistic corrections are only a few percent at the highest momenta shown). From an inspection of the curves in Fig. 6, it is evident that curves C and F definitely disagree with the experimental results. The conclusion reached by Henley (see Sec. I) that the Chew-Goldberger momentum distribution contains too many high momentum components is thus also verified by this experiment. Although curve D seems to give the best fit to the data, curve E is not in violent disagreement. In fact, any Gaussian nucleon momentum density distribution with a $1/e$ value between 14 and 19 Mev would not be inconsistent with the experimental results.

Differential cross sections of protons from deuterium are obtained by comparing the proton yields from deuterium to the corresponding yields from hydrogen as described before. These cross sections, together with the 30° and 40° p-p cross sections at 340 Mev and n-p cross sections at 270 Mev, are listed in Table I. It is seen that the cross sections of protons from deuterium nearly equal the sum of the proton-nucleon cross sections. Because of the internal momenta involved in the case of protons from deuterium, the cross sections obtained represent averages over proton-nucleon collisions in particular ranges of relative energies and scattering angles, where the scattering angles are considered measured from the direction of approach of the interacting nucleons in the center-of-mass system to the direction of observation in the laboratory system. The condition mentioned above concerning the cross sections is considered plausible since (1) interference effects at the scattering angles used are small, (2) the nucleons of the deuteron are much of the time so widely separated with respect to the De Broglie wavelength of the bombarding protons that they may act as independent scattering centers, (3) the ranges of relative nucleon energies and scattering angles mentioned above are small in comparison with their mean values, (4) the free proton-nucleon cross sections are not sensitive functions of the energy at 340 Mev, and (5) the free proton-proton differential cross section, which is larger than the corresponding proton-neutron cross section at the scattering angles used, has a flat angular dependence in the c.m. system so that its variation in the laboratory system goes only as the cosine of the scattering angle.

The data from carbon does not give information concerning cross sections since the entire spectra were not obtained. However, the extrapolated spectral curves indicate that the proton yields may be close to those predicted by the corresponding free proton-nucleon collision cross sections. Furthermore, the proton spectrum from oxygen at 40° (see Fig. 8) is well represented by a curve obtained by multiplying the theoretical spectrum from carbon by 16/12. A 30° proton spectrum from oxygen was not obtained because deuterated paraffin was used instead of heavy water to supply deuterons at this angle.

Finally, it must be stated that the theoretical spectral curves have been arbitrarily translated along the energy scale toward lower energies in the case of carbon, in order that they may fit the data. On the basis of the simple mechanical calculations, the peaks of the energy spectra from deuterium, carbon, and oxygen should fall at the peaks of the spectra from hydrogen. Figures 4 and 5 indicate that they not only fail to coincide but also that the energy differences of the peaks seem to increase with the scattering angle. To be sure, the proton-nucleon cross sections favor small relative energy collisions, but this effect accounts for only a few Mev of the energy

TABLE I. Total differential cross sections in the laboratory system.

Scattering angle	p-$p^{a}\times10^{27}$	p-$n^{b}\times10^{27}$	p-$d\times10^{27}$
30°	13.2	7.3	15.7±1.8
40°	11.6	2.1	12.8±0.6

[a] Obtained by Chamberlain *et al.* (see reference 15) using 340-Mev proton beam.
[b] Obtained by Kelly *et al.* (Phys. Rev. 79, 96 (1950)) using 270-Mev neutron beam.

differences observed. The greater portions of these energy differences are undoubtedly due to nuclear effects, such as the nuclear potential well and the binding and excitation energies, which have not been considered in the calculations. It is difficult to account for these effects in a quantitative manner, but rough calculations show that the energy differences observed should be expected.

First, it is easily seen that the nuclear potential well (the negative potential energy the incident proton experiences in the nucleus due to the proximity of all of the nucleons except the nucleon with which the proton collides) reduces the average proton energy observed from the value expected from free proton-nucleon collisions. A proton having an initial energy E_0 and being scattered an angle θ by a free nucleon initially at rest will have an energy E that is given nonrelativistically by the expression,

$$E=E_0\cos^2\theta.$$

In the case of a proton being scattered by a nucleon that is bound in a nucleus, the energy E_0 must be augmented by the average nuclear well depth V_0. After colliding with a nucleon and before leaving the nucleus, this energy V_0 must be relinquished by the proton. The peak of the energy distribution due to this cause would roughly fall at an energy

$$E=(E_0+V_0)\cos^2\theta-V_0=E_0\cos^2\theta-V_0\sin^2\theta.$$

The energy differences predicted ($V_0\sin^2\theta$) are seen to be dependent on the scattering angles. If V_0 is taken to be 30 Mev, then the differences are 7.5 Mev at 30° and 12.4 Mev at 40°. The observed differences are about 12 Mev at 30° and 27 Mev at 40°. Nuclear rearrangements that accompany quasi-elastic processes are considered to account for the remainder of the energy differences observed. When a 340-Mev proton is scattered by a nucleon to an angle greater than about 25°, the momentum imparted to the nucleon is so great that it too may leave the nucleus. If both the proton and the nucleon escape from the nucleus with no further encounters, then the excitation energy of the nucleus would probably be small, but the binding energy of the nucleon in the nucleus must be provided for the nuclear transition involved to take place. Since this energy must be subtracted from the nucleons which are to leave the nucleus, the average energy of the quasi-elastically scattered protons is reduced. Since the binding energy of a neutron in C^{12} is as high as 20 Mev, these considerations are probably sufficient to account for the observed energy differences in the peaks of the spectra.

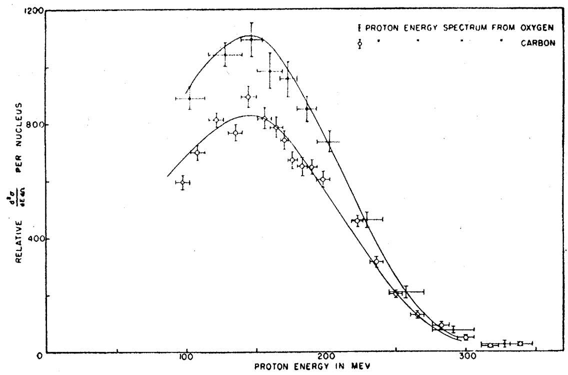

FIG. 8. Proton energy spectra at 40° from 340-Mev protons on carbon and oxygen. The ordinates of the theoretical curve drawn to the data from oxygen are greater than those of the corresponding carbon curve by a factor of 16/12.

VI. ACKNOWLEDGMENTS

The authors wish to express their gratitude to Dr. James Hadley for originally designing the components of the particle spectrometer and for frequent suggestions concerning its used. Mr. John Wilcox assisted appreciably during the runs. The authors are also indebted to Dr. Peter A. Wolff for enlightening discussions concerning the interpretation of the results. Finally, thanks are due to members of the cyclotron crew who skillfully supplied the steady proton beam current, to the accelerator technicians who assisted before each run in the enlargement of the cave that was necessary to accommodate the particle spectrometer, and to the electronics maintenance men who patiently kept the extensive associated electronics equipment in good operating condition.